

DIAGNOSTICS BEAMLINE OPTIMISATION AND IMAGE PROCESSING FOR SUB-PS STREAK CAMERA BUNCH LENGTH MEASUREMENT

C.A. Thomas*, I. Martin, G. Rehm, Diamond Light Source, Oxfordshire, UK

Abstract

For the low-alpha beam mode at Diamond, standard theory predicts rms bunch lengths as small as 0.6 ps with a momentum compaction factor set to $\alpha = 0.8 \cdot 10^{-6}$. In order to be able to reliably measure such a short bunch, we have been optimising the optical design of the visible diagnostics beamline, and we have implemented image processing to take into account the point spread function of the streak camera. The optical design has reduced a large chirp of 15 ps to less than 2 ps over the 400-550 nm bandwidth. It has also permitted the transport of almost all the available power, increasing the power by a factor 30, yet maintaining the possibility to focus the beam down to less than 20 μm into the streak camera for the best static streak camera point spread function. The implemented de-convolution technique extends the performance of the streak camera to bunch length measurements of less than the 1 ps PSF of the streak camera. In this paper we present these two essential features required to measure sub-ps bunches with a streak camera.

INTRODUCTION

For the low-alpha beam mode at Diamond, rms bunch lengths based on synchrotron frequency measurement are calculated to be as small as 0.6 ps. In special user low alpha beam mode the bunch length is set to be of the order of 2.5 ps. Measuring such small bunch lengths reliably can be quite challenging. For such a measurement we use a streak camera¹ (SC), for which the resolution as defined using the Rayleigh criterion and specified by the manufacturer is 2 ps (measured using narrowband pulses with a few photons per pulse). The corresponding rms resolution is then 0.75 ps. This should allow the SC to be able to measure bunch lengths 2 ps or less. However, control of the bandwidth and the power of the photon pulse is fundamental: too much power will induce Coulomb explosion of the electron bunch in the streak tube, and thus measurement of a longer bunch. Too little power will render the measurement dependant on the jitter of the many pulses needed to form an image.

In addition to this, one needs to take into account the possible chirping of the pulse going through various lengths of glass. To reach the photocathode of the SC, a pulse passes through at least the 4.3 mm of quartz on the entry of the SC tube. In our case there is also 6.3 mm of fused silica from a vacuum-air separation window. But the beam

needs to be transported and focussed onto the photocathode, and the use of lenses will cause any broadband pulse to be chirped, potentially becoming longer than the electron bunch length that generated it. This is what we called the dynamic point spread function of the SC [1]. It is measurable with the time resolved spectrum of the pulse which shows the length and centroid of the pulse as function of the spectrum. With the original refractive focussing optics a non-linear chirp of 15 ps over 150 nm bandwidth with a maximum gradient of 140 fs/nm was measured. This chirp induces a dynamic point spread function rms width of approximately 6.5 ps. Re-designing the focussing optics using mirrors reduced this chirp to less than 2 ps for the same 150 nm bandwidth, with a maximum gradient 30 fs/nm [2]. Control of the power and bandwidth of the pulse is a first step, but with bunch lengths equal or less than the static PSF width, a very accurate knowledge of the PSF is absolutely necessary to allow the deconvolution and so recover the original bunch profile.

In this paper, we present which conditions are necessary for the measurement of ps bunch lengths. We first present the optical design of the Diagnostics beamline which allows the focussing of an un-chirped pulse with almost all the available power from the bending magnet synchrotron radiation onto the SC photocathode. Then we briefly introduce the Lucy-Richardson image deconvolution technique applied to the SC images. Finally, before some concluding remarks we show measurement of ps bunch lengths after the optimisation and deconvolution technique presented previously has been applied.

OPTICAL DESIGN

The improvement of the performance of the SC goes in two steps. The first one is the re-design of the front focusing optics (FO), replacing the achromatic Nikkor lens by an assembly of mirrors (Fig. 1). The second one is a re-design of the beam transport from the source to the SC with the aim to transport the maximum available power. The new design collimates the beam and reduces its transverse size at the same time, in order to transport the geometrical beam through the 30x50 mm aperture of the chicane in the radiation shield wall. A layout of the design is shown in Fig. 3.

Streak Camera Reflective Front Optics

The main objective of replacing the reflective FO of the SC by a refractive FO is to suppress the chirp induced by the refraction index of the objective lens in the broad spectrum synchrotron radiation pulse. This way all the UV-visible power spectrum can be used for bunch length mea-

* cyrille.thomas@diamond.ac.uk

¹Optronis GmbH

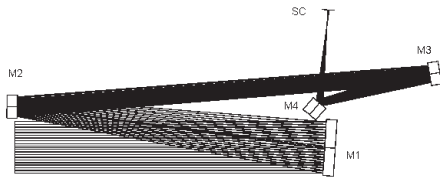


Figure 1: Drawing of the reflective FO assembly. Mirror M1 is parabolic concave, M2 is spherical convex, M3 is spherical concave, M4 is flat. The footprint of the assembly is smaller than an A4 sheet of paper.

Table 1: PSF Width of the SC with the Refractive and the Reflective Optics

	Reflective Optics	Refractive Optics
σ (pixel)	6.2	6.3
σ at 15 ps/mm (ps)	1.07	1.08
σ at 25 ps/mm (ps)	1.93	1.94
σ at 50 ps/mm (ps)	3.92	3.95

surement without the need of reducing the bandwidth and thus the power of the incoming pulse. The design of the FO has been done using ZEMAX software, looking at the focussing performance of the assembly. The result showed the possibility to focus the astigmatic synchrotron radiation beam in a $10 \times 20 \mu\text{m}^2$ spot. The experimental verification is shown in Fig. 2, where the synchrotron radiation is focussed on the SC with both FO. The PSF of the SC as shown in Table 1 is comparable in both cases.

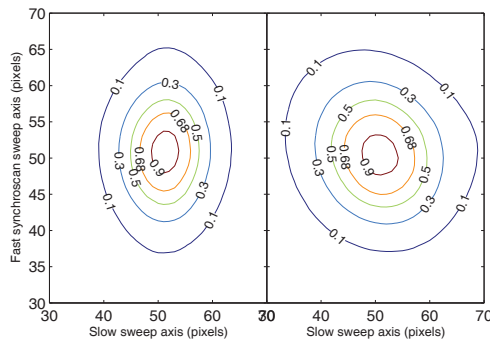


Figure 2: SC PSF measured with both refractive (left) and reflective FO (right).

Beamline Transport Design

The original design of the diagnostics visible beamline is shown in Fig. 3. For several reasons including simplicity of alignment, robustness and cost, the design included only flat mirrors of 50 mm diameter. The calculated geometrical factor power loss, due to the divergence of the beam, was of the order of 20 to 30, and the additional loss through the reflectivity of the mirrors is 43% - each of the 8 mirrors with UV-enhanced Al coating providing 90% average reflectiv-

ity over the range 350-650 nm. In spite the power loss, the SC could be operated with the fastest sweep, recording images of a single turn, but only with the full power available.

In order to transport all the synchrotron radiation power reflected by the first mirror (mirror [a] in Fig. 3), we designed a Z-fold mirror assembly, composed of a concave parabolic and a convex spherical mirror ([I] and [II] in Fig. 3), which collimates the synchrotron radiation beam and reduces its transverse size by a factor ≈ 7 . Also we changed mirrors [b] and [c] for larger diameter ones (76 mm). This should recover the geometrical loss from the original design, but may bring power loss through the additional two reflections. For that we decided to change the coating to dielectric multilayer, which provides an average 99% reflectivity over the bandwidth 400-750 nm. The total power loss by reflection over 10 mirrors is expected to be 90%. Measurements performed with and without the Z-fold assembly confirmed the prediction: with a filter at 550 nm the power with the Z-fold assembly is approximately 30 times larger than without the Z-fold. With this power, the SC can acquire images of a single bunch in single shot with reduced bandwidth.

IMAGE DECONVOLUTION

In order to deconvolve the SC images, one needs to measure or to know perfectly the PSF of the instrument. We can measure the PSF at the time of the experiment by switching off the sweep electrodes of the SC as shown in Fig. 2. Using the implementation of the Lucy-Richardson [3, 4] algorithm in Matlab, we directly supply the measured PSF to deconvolve the SC images. Not detailing the algorithm, its main characteristics are that it is an iterative converging algorithm, and the noise on the image is assumed to be Poisson distributed. These two features makes this algorithm appropriate to the deconvolution of SC images. A demonstration is shown below where we acquired SC images of the Diamond bunches with a Low Alpha lattice, and in which we varied the momentum compaction factor from 0.8 to $6.8 \cdot 10^{-6}$, expecting the bunch length to vary from 0.6 ps to 1.9 ps. The RF cavity voltage was kept constant at 3.4 MV. There were 900 bunches stored with an average current of 1.6 μA .

BUNCH LENGTH MEASUREMENT

Knowing that the pulses with 400-650 nm bandwidth have a 2 ps chirp, we restricted it to less than 0.3 ps by selecting the 550 ± 20 nm bandwidth of the pulse to be measured with the SC. We measured the PSF by switching off the sweep electrodes of the SC. The image is similar to the one shown in Fig. 2. We set the momentum compaction factor (α) and indirectly measured it by measuring the synchrotron frequency. For each value of α set, 10 SC image were acquired. The analysis performed on the SC images was, firstly, a Gaussian fit was performed on 13 slices across each image, then each image was deconvolved

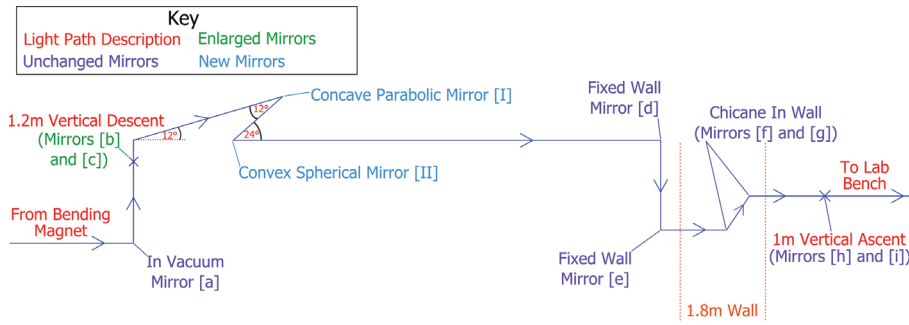


Figure 3: Design of the optical transport beamline. The total path length is ≈ 25 m. The original design includes mirrors [a] to [i], and the new design the addition of the Z-fold assembly, mirrors [I] and [II].

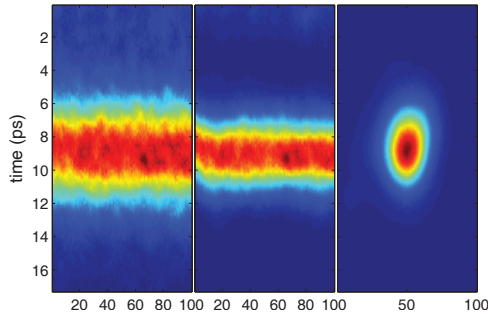


Figure 4: SC images: Left, raw image with $\alpha \approx 1.210^{-6}$; Middle, same image but deconvolved; Right, SC PSF. Horizontal axis represents the slow axis sweep set to 500 $\mu\text{s}/\text{mm}$. On each image a region of interest of 100×100 pixels is selected, equivalent to ≈ 17 ps \times 600 μs .

and a Gaussian fit performed on the same slices over each deconvolved image. An example of the deconvolved image is shown in Fig. 4. The result of the Gaussian fit for all the values of α is shown in Fig. 5. An estimate of the bunch length can be calculated using the quadratic subtraction of the width given by the raw image Gaussian fit by the width of the PSF, also fit with a Gaussian. In order to compare the results, the theoretical near zero current bunch length is also shown in the figure. One first notes that the raw image is nearly a factor 2 larger than the theoretical value, and between 30% and 100% larger than the PSF width. The width of the deconvolved images is closer to the theoretical near zero current value, 10% to 20% for most of the measured points, but gets 90% larger for the smallest values of α . The bunch length obtained from the quadratic subtraction is of course smaller than bunch length from the raw image, but as observed it doesn't come close to the deconvolved image bunch lengths.

Several explanations can be brought to explain the difference to the theoretical predictions. The first one can be random jitter of all the 900 bunches, due to synchrotron oscillation of individual bunches. During all the time of the experiment, relatively strong synchrotron oscillation were observed, which might support this first hypothesis. Another explanation might come from RF cavity high

frequency noise which can also excite randomly all the bunches through their energy spread. Another explanation is of course the deconvolution didn't converge to the expected value. However, from the many tests through simulation we performed with this deconvolution algorithm, we always recovered the bunch length, even with very noisy images. We also note other theoretical limits are placed on the minimum bunch length which have not been taken into account. For instance, RF voltage phase noise through dispersion can contribute to the longitudinal bunch distribution, the same way as the quantum excitation [5]. Path length dependance on the betatron motion could also contribute to the bunch length, as described in [6]. These possible contributions to the minimum bunch length need to be evaluated numerically, and perhaps also measured.

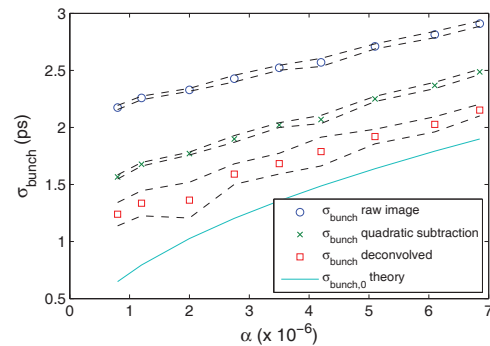


Figure 5: Bunch length measured as function of α . The dashed lines represent the standard deviation over the set of 10 images with 13 slices per image per measurement point. The mean value of the bunch length is shown for the fit of the raw images, the deconvolved images, and also for the quadratic subtraction using the width of the PSF, $\sigma_{PSF} = 1.5$ ps. The solid line is the expected theoretical near zero current bunch length value.

CONCLUDING REMARKS

We have shown the technique and setup of a streak camera to be able to measure bunch length of ≈ 1 ps. The pulse to be measured should contain the most available power,

but also the minimum chirp induced by the material it has traversed. To achieve this, we had to re-design the SC front optics, but also the transport beamline. We then could afford to lose some power by filtering the pulse bandwidth in order to control the residual chirp. The resulting performance is a PSF width of 1 ps. Extremely small bunch length in the 1 ps range could be measured with the SC in the optimum condition, and also using a deconvolution technique.

REFERENCES

- [1] C. A. Thomas, I. Martin, and G. Rehm. Investigation of extremely short beam longitudinal measurement with a streak camera. In *Proceedings of DIPAC 2009*, pages 260–262, May 2009.
- [2] C. A. Thomas, I. Martin, and G. Rehm. Performance of a streak camera using reflective input optics. In *Proceedings of IPAC 2010*, pages 1170–1173, May 2010.
- [3] W. H. Richardson. Bayesian-based iterative method of image restoration. *J. Opt. Soc. Am.*, 62(1):55–59, Jan 1972.
- [4] L. B. Lucy. An iterative technique for the rectification of observed distributions. *Astronomical Journal*, 79:745, jun 1974.
- [5] S. Daté, K. Soutome, and A. Ando. Equilibrium bunch length with rf noises in electron storage rings. *Nuclear Instruments and Methods in Physics Research A*, 355:199–207, feb 1995.
- [6] Y. Shoji. Dependence of average path length betatron motion in a storage ring. *Phys. Rev. ST Accel. Beams*, 8:094001, Sep 2005.